Research Article

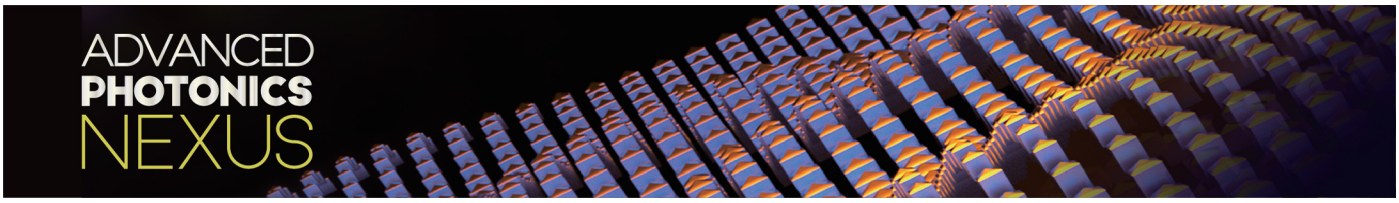

Achieving high-security and massive-capacity optical communications based on orbital angular momentum configured chaotic laser

Yanwei Cui,[a] Jianguo Zhang,[a,*] Zhongquan Nie,[b,*] Anbang Wang,[c,d,*] and Yuncai Wang[c,d]

[a]Taiyuan University of Technology, Ministry of Education, College of Electronic Information and Optical Engineering, Key Laboratory of Advanced Transducers and Intelligent Control System, Taiyuan, China
[b]National University of Defense Technology, College of Advanced Interdisciplinary Studies, Changsha, China
[c]Guangdong University of Technology, School of Information Engineering, Guangzhou, China
[d]Guangdong Provincial Key Laboratory of Photonics Information Technology, Guangzhou, China

Abstract. Secure and high-speed optical communications are of primary focus in information transmission. Although it is widely accepted that chaotic secure communication can provide superior physical layer security, it is challenging to meet the demand for high-speed increasing communication rate. We theoretically propose and experimentally demonstrate a conceptual paradigm for orbital angular momentum (OAM) configured chaotic laser (OAM-CCL) that allows access to high-security and massive-capacity optical communications. Combining 11 OAM modes and an all-optical feedback chaotic laser, we are able to theoretically empower a well-defined optical communication system with a total transmission capacity of 100 Gb/s and a bit error rate below the forward error correction threshold 3.8×10^{-3}. Furthermore, the OAM-CCL-based communication system is robust to 3D misalignment by resorting to appropriate mode spacing and beam waist. Finally, the conceptual paradigm of the OAM-CCL-based communication system is verified. In contrast to existing systems (traditional free-space optical communication or chaotic optical communication), the OAM-CCL-based communication system has three-in-one characteristics of high security, massive capacity, and robustness. The findings demonstrate that this will promote the applicable settings of chaotic laser and provide an alternative promising route to guide high-security and massive-capacity optical communications.

Keywords: chaotic secure communication; orbital angular momentum configured chaotic laser; high security; massive capacity; misalignment.

Received Apr. 15, 2024; revised manuscript received May 24, 2024; accepted for publication Jun. 4, 2024; published online Jun. 27, 2024.

[DOI: 10.1117/1.APN.3.4.046008]

1 Introduction

Chaotic laser can effectively ameliorate the problem of insufficient security of optical communications due to its noise-like and high-bandwidth characteristics.[1–3] However, there are three key challenges in secure optical communications based on the chaotic laser: (i) because of the limited bandwidth of the chaotic laser, their security performance will degrade significantly in high-speed optical communications; (ii) the current rate of chaotic optical communication systems is mostly in tens of Gb/s, thus failing to satisfy the actual communication needs of hundreds of Gb/s; and (iii) the existing methods of chaotic optical communication do not take into account the spatial expansion of chaotic laser, which is difficult to support multidimensional superior security and high-density storage. Therefore, there is an urgent demand to develop a technology that combines spatial modes with chaotic lasers to achieve high-security and massive-capacity optical communications.

*Address all correspondence to Jianguo Zhang, zhangjianguo@tyut.edu.cn; Zhongquan Nie, niezhongquan1018@163.com; Anbang Wang, abwang@gdut.edu.cn

Numerous efforts have been dedicated to the development of enhanced bandwidth[4–10] and expanded capacity[11–16] in the chaotic laser empowered communication systems. It has been shown, for the former, that the use of extra optical injection,[4,5] tunable optical feedback,[6,7] efficacious postprocessing,[8,9] etc. enables to boost the safety of information. However, the realization of increased bandwidth with these strategies is at the cost of cumbersome chaotic laser structure, which is not beneficial to real optical communication applications. For the latter, by leveraging orthogonal frequency-division multiplexing,[11] polarization-division multiplexing,[12] and wavelength-division multiplexing,[14] it permits one to effectively enlarge capacity of the chaotic secure optical communication systems. Yet, these methods only allow capacity in tens of Gb/s, impeding extremely large capacity optical communication. It is thus highly desired to incorporate a fire-new dimension into the chaotic laser, which can not only enhance the security of the optical communication system but also impressively improve the communication capacity. Over the past decade, spatial orbital angular momentum (OAM), which is carried by optical vortices with the helical transverse phase structure of $e^{il\phi}$ (ϕ is the transverse azimuthal angle, and l is the topological charge), has aroused unprecedented research enthusiasm in optical communication,[17–25] optical manipulation,[26] optical trapping,[27,28] optical storage,[29] optical detection,[30,31] and high-resolution imaging.[32,33] Particularly in optical communication, the OAM offers a promising prospect on account of its additional confidentiality, infinite orthogonal modes, environmental insensitivity, and good compatibility. Therefore, an interesting question arises: whether it is possible to fuse temporal chaotic laser with spatial OAM to realize high-security and massive-capacity optical communication?

Here, we introduce a conceptual paradigm to yield orbital angular momentum configured chaotic laser (OAM-CCL), which can be used to achieve a high-security and large-capacity optical communication system. Specifically, on the one hand, it is found that the OAM-CCL-based communication system still maintains the high security even at low optical signal-to-noise ratio (OSNR, 20 dB) and complete eavesdropping. On the other hand, by utilizing 11 orbital angular momentum modes, the OAM-CCL-based communication system is theoretically expected to realize a communication rate of 100 Gb/s. It means that the potential degrees of freedom (>100) of the system still allow a higher communication capacity (>100 Gb/s) with a bit error ratio (BER) below the forward error correction (FEC). Moreover, the robustness of the OAM-CCL-based communication system to misalignment is revealed. Finally, we validate the conceptual paradigm of the OAM-CCL-based communication system. In brief, all the above superiorities indicate that the OAM-CCL-based communication system not only alleviates the drawback that the security of the traditional OAM communication system cannot be fully guaranteed but also solves the issue of limited transmission capacity in traditional chaotic secure optical communication. Our study will help promote the application of chaotic lasers in multidimensional, high-security, massive-capacity, and robust optical communication.

2 System Model Setup

2.1 OAM Configured Chaotic Laser

In order to tackle the shortcomings of the traditional chaotic laser, we propose a conceptual paradigm of OAM-CCL, as shown in Fig. 1(a). After OAM configured, the wavefront of the chaotic laser becomes a helical structure, and the temporal properties of the chaotic signal are preserved. Thus the OAM-CCL can be used as a broadband chaotic laser source driving a pair of lasers to generate synchronous masking signals for communication in free space. The OAM-CCL is schematically shown in Fig. S1 in the Supplementary Material. The OAM-CCL possesses the following characteristics: (i) it is difficult to eavesdrop in free space, providing additional security. (ii) It can be spatial quadrature multiplexed with other OAM beams, bringing additional freedom to the optical communication system, similar to Fig. 1(b).

2.2 OAM-CCL-Based Communication System

The schematic diagram of the communication system based on OAM-CCL is shown in Fig. 2. An all-optical feedback chaotic laser SL_D with a wavelength of 1550 nm generates a high-bandwidth chaotic laser as the driving chaotic source.[34] The driving chaotic signal is split into two parts: one part is injected into the laser SL_T to generate an encrypted chaotic signal $E_{ch}(t)$, whereas the other part is sent to the receiver and injected into SL_R to generate a synchronous chaotic signal $E'_{ch}(t)$.[35] Continuous-wave lasers $SL_1 - SL_{10}$ are modulated to produce 10 Gb/s nonzeroing on–off keying signals $E_n(t)$, respectively. After that, the information signals are masked as encrypted signals $E_n^{enc}(t) = E_n(t) + aE_{ch}(t)$. Note that due to the presence of the attenuator the masking coefficients differ from channel to channel, avoiding the possibility of the eavesdropper removing the chaotic signal by simple differencing.

Then the encrypted signals are coupled from single-mode fibers to free space via collimators that can be described as Eq. (S1) in the Supplementary Material. After the construction of spatial light modulators, the beams carrying the encrypted signals is, respectively, converted into vortex beams of OAM ±3, OAM ±5, OAM ±7, OAM ±9, and OAM ±11, as shown in Eq. (S2) in the Supplementary Material. Similarly, the driving chaotic signal is also converted from a Gaussian beam to an OAM +1 beam, multiplexed with other encrypted signals through beam splitters and transmitted to the receiver via free space, which can be described as Eq. (S3) in the Supplementary Material. At the receiver, the multiplexed OAM beams are subjected to an opposite topological charge and filtered to demultiplexing, the optical field can be expressed as Eq. (S4) in the Supplementary Material. The demultiplexed driving chaotic signal will be injected into the laser SL_R to generate synchronous chaotic signal $E'_{ch}(t)$. The demultiplexed encrypted signals are differenced from the synchronous chaotic signal to recover information signals $E'_n(t) = E_n^{enc'}(t) - a'_n E'_{ch}(t)$.

The commonly driven chaotic synchronization mechanism is used in the OAM-CCL-based communication system.[36,37] This scheme has the advantages of simplicity, robustness, fast synchronization, and suitability for multichannel encryption. When the driving chaotic signal is injected into a pair of parameter matching slave lasers with a certain intensity, the two slave lasers will produce highly synchronous chaotic signals for encryption and decryption. We use Eqs. (S5)–(S7) in the Supplementary Material to describe the complex chaotic synchronization dynamics and stable spatial modes in the OAM-CCL optical communication system.

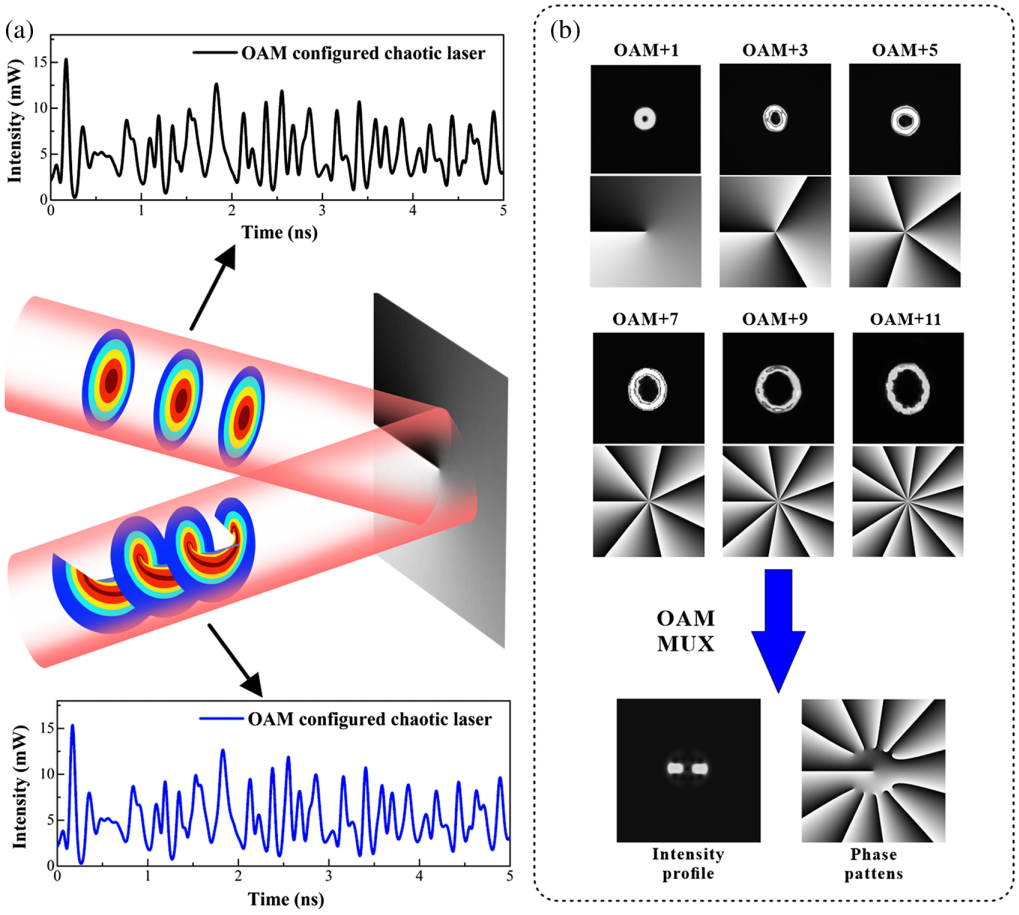

Fig. 1 OAM-CCL. (a) Concept of OAM-CCL and (b) intensity profiles and phase fronts for different OAM beams.

3 Result

3.1 Multidimensional High Security

The OAM-CCL-based communication system inherits the security of traditional chaotic secure optical communication. Figure 3 shows the simulation results of the OAM-CCL-based communication system in the time domain. Figure 3(a) shows the time waveform of the chaotic lasers SL_D, SL_T, and SL_R. The synchronization coefficient of the two slave lasers SL_R and SL_T is 0.976, and the synchronization coefficient between the driving laser SL_D and the slave laser SL_T is 0.763, which means that attackers cannot use the driving chaotic signal for decryption, ensuring the security of the system. The effective bandwidths (80% energy) for driving and masking chaotic signal are 11.73 and 13.35 GHz, respectively. Figure 3(b) shows the variation of the power spectrum of the information signal before and after encryption with $\rho = 0.187$. The masking coefficient ρ is defined as the ratio of the amplitude of the information signal to the amplitude of the chaotic signal.[38] The encrypted signal exhibits a noticeably flat power spectrum, indicating effective masking of the information signal by the chaotic signal. In Fig. 3(c), the impact of different masking coefficients on the BER is shown for both legitimate and illegitimate decryption at an OSNR of 20 dB. It can be seen that even if the signal is completely eavesdropped, the system still achieves secure communication within a masking coefficient range of 0.31 to 0.56. In Fig. 3(d), the BER for legitimate decryption of the system is presented. It can be observed that increasing the masking coefficient enhances the system's tolerance to noise, but it may reduce the system's security level.

In addition to the conventional temporal domain security discussed above, the OAM-CCL communication system also demonstrates remarkable resistance against eavesdropping in the spatial domain. These outcomes are elucidated further in Sec. S5 of the Supplementary Material. We substantiate this eavesdropping resilience by constructing an eavesdropping channel. Our results indicate that compared to the free-space optical communication system, Eve's eavesdropping on the OAM-CCL-based communication system for high-quality interception requires a larger size and positioning closer to the optical axis. In this case, Eve's interception of the beam at such a close position will cause Bob's alarm.

3.2 Massive Capacity with Compatibility

For the OAM-CCL-based communication system, the limit value of communication rate C_{lim} can be described as Eq. (S9) in the Supplementary Material. The parameters C_{max} and DoF determine the value of C_{lim}, which represents the system single-mode maximum rate and the system degree of freedom, respectively. C_{max} is related to the bandwidth of the chaotic carrier and masking coefficient.[39] Figure S6 in the Supplementary Material shows the relationship between a

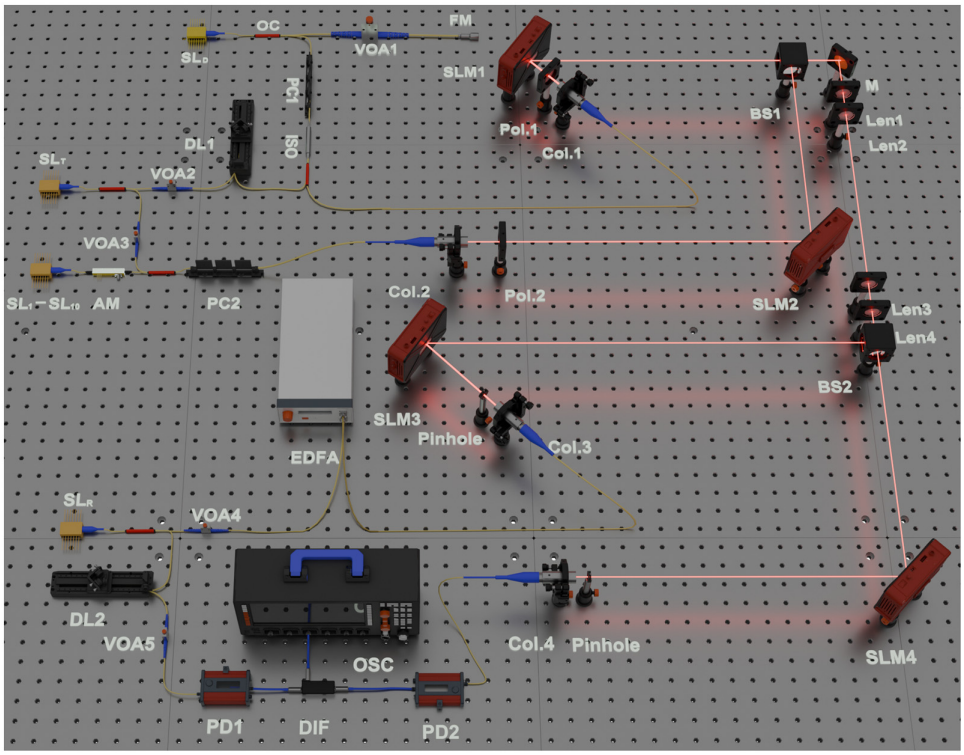

Fig. 2 Schematic diagram of the communication system based on OAM-CCL. SL, laser; VOA, variable optical attenuator; FM, fiber optic mirror; PC, polarization controller; DL, delay line; Col., collimator; Pol., linear polarizer; SLM, spatial light modulator; EDFA, erbium-doped fiber amplifier; AM, amplitude modulator; BS, free-space beam splitter; M, mirror; PD, photodetector; DIF, current differential; and OSC, oscilloscope.

single-mode information rate and BER for the system with different masking coefficients at OSNR = 20 dB. The relationship between the mode number and the system capacity of the system with different masking coefficients is shown in Fig. 4(a). It is clear that the communication rate increases in proportion to the mode number.

Theoretically, OAM modes have infinite degrees of freedom, but in practice, because of the divergence nature of OAM beams, the degrees of freedom of the system are limited under finite physical conditions. Here, we modify the study result of Sawan et al.[40] and considering the beam limitation by the transmitter, define the DoF for the OAM-CCL-based communication system:

$$\mathrm{DoF} \triangleq \max_{\omega_0} \#\left\{ \mathrm{LG}_p^l | r_p^l(0) \le R_T, 1 - \frac{R_R^2}{z^2 + z_R^2} \le \mathcal{P} \right\}, \tag{1}$$

where #{} represents the size of a set, r_p^l indicates the beam size,[41] R_T denotes the transmitter radius, and R_R denotes the receiver radius. $\mathcal{P}$ is the paraxial estimator, and it is the ratio of the true power crossing a transverse area obtained using the Helmholtz and paraxial equations. [42] The paraxial estimator not only can be used to indicate the validity of paraxial approximation of the beam but also the beam divergence. The higher-order OAM modes have a smaller paraxial estimator, so the paraxial estimator can be used as an important parameter for defining the DoF. Equation (1) defines a degree of freedom as the set of all LG modes that satisfy a beam emission size smaller than the emitter size and an estimate of the beam evening axis at the receiving end greater than the reference value. The paraxial estimator and beam size are calculated as shown in Sec. S13 in the Supplementary Material.

Figure 4(b) shows the relationship between transmission distance and DoF for different initial beam waists, as the transmission distance increases, the DoF tends to decrease. At close range (<345 m), the smaller the initial beam waist is, the higher the DoF in the system is, and the opposite is true at long range. And the receiver size plays a role in constraining the degrees of freedom, as depicted in Fig. S7 in the Supplementary Material. Therefore, in order to ensure the freedom of the system, the appropriate transmitter size, receiver size, and initial beam waist radius should be selected depending on the communication distance.

3.3 Optimizable Misalignment Robustness

In practical applications, mechanical vibrations and wind variations can cause minor displacements or jitters, which may cause misalignment between the transmitter and receiver. Such a misalignment leads to a decrease in orthogonality between OAM modes,[43–47] thus giving rise to a deterioration of chaotic synchronization and communication quality in the OAM-CCL-based communication system. The basic forms of misalignment include angular error and displacement error between the transmitter and the receiver, shown as Fig. S10 in the Supplementary Material.

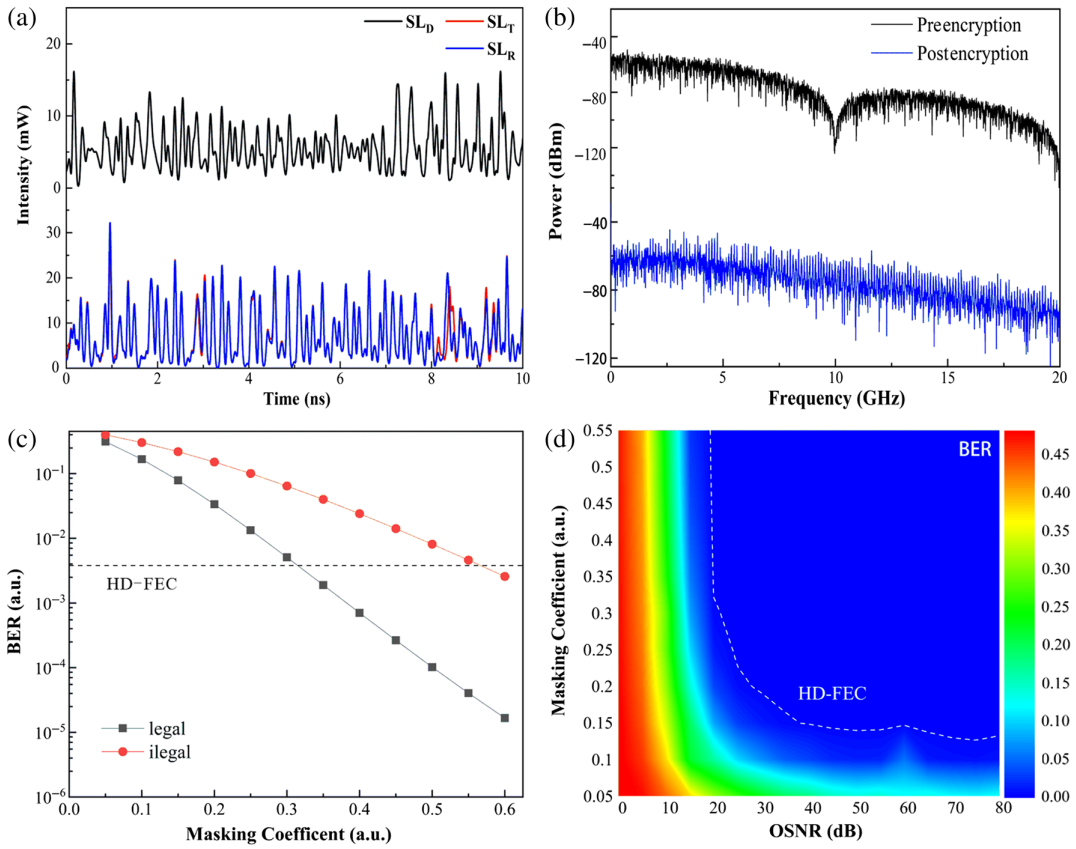

Fig. 3 System performance. (a) Timing waveforms of SL_D, SL_T, and SL_R; (b) power spectrum before and after encryption; (c) BER versus masking coefficient at OSNR = 20 dB; and (d) BER versus masking coefficient at different OSNRs.

By adjusting the basic parameters, we find that the OAM-CCL-based communication system exhibits robustness to misalignment. Figure 5(a) shows the variation of the synchronization coefficient when displacement error and angle error occur simultaneously. Figure 5(b) shows the BER variation with a mode spacing of 2 under the presence of displacement error and angular error, when $\rho = 0.187$, $\omega_0 = 2$ cm. Beyond that, we have also investigated the change in system performance when displacement and angular errors occur independently, and the specific results are shown in Figs. S11–S14 in the Supplementary Material. We find that the larger the beam waist is, the more robust the system is to displacement error, and the less robust it is to angular error. Larger mode space can reduce the crosstalk between modes, but it may increase the overall

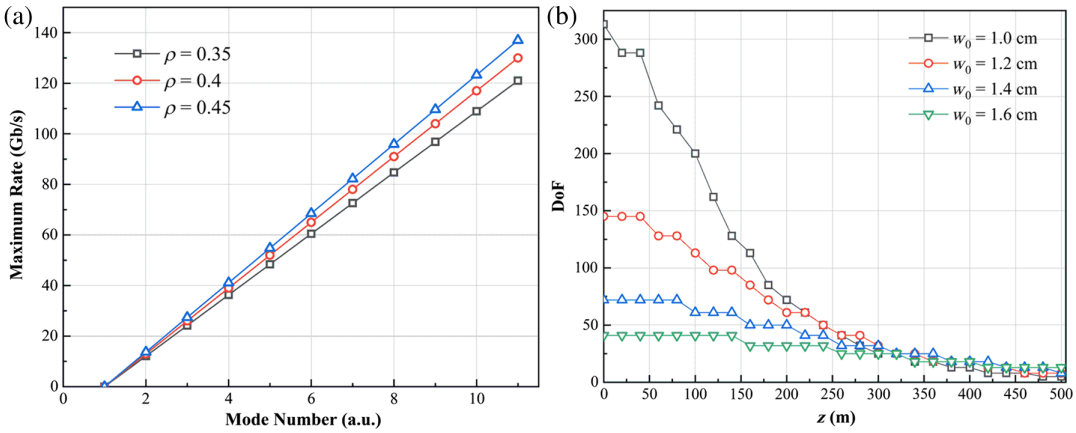

Fig. 4 System capacity and degrees of freedom. (a) System capacity versus mode number for different masking coefficients at OSNR = 20 dB. (b) The relationship between receiver size and transmission distance for different beam waists, $R_R = 10$ cm and $R_T = 10$ cm.

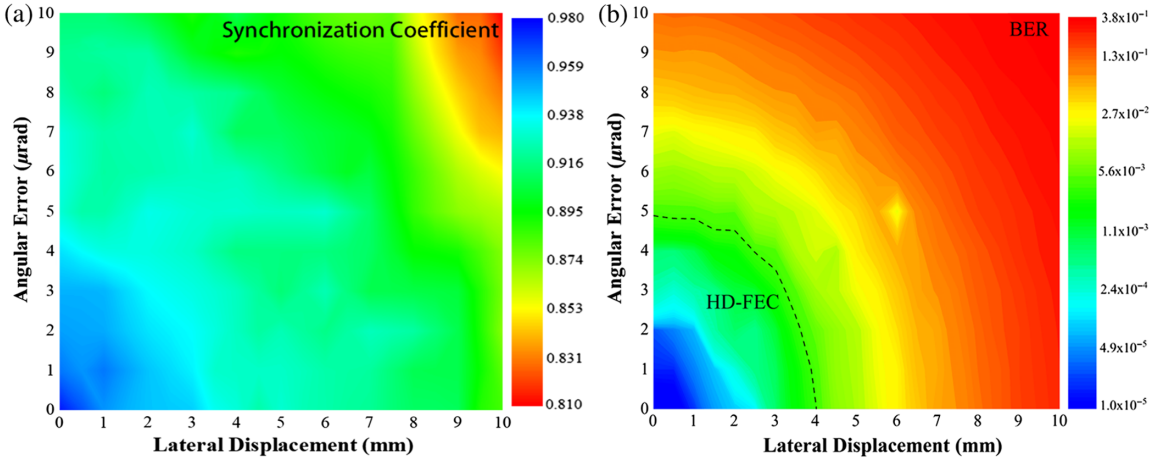

Fig. 5 System performance with misalignment. (a) Synchronization coefficient under simultaneous displacement and angular errors. (b) BER of OAM +3 mode under simultaneous displacement and angular errors, with $\rho = 0.187$, $\omega_0 = 2$ cm, and mode space = 2.

power loss of the system. Therefore, the choice of initial beam waist and mode space should be carefully considered in the system design.

3.4 Discussions and Prospects

As a conceptual illustration, we built a prototype system of OAM-CCL-based communication system, as shown in Fig. 6. The prototype system is used to simulate image transfer experiment, and the simulations together confirmed the above conclusions, as detailed in Sec. S11 in the Supplementary Material. More interestingly, the OAM-CCL, as a new type of hybrid laser, is in a position to realize the coupling of temporal chaotic laser and spatial OAM in an all-optical way, which means that more dimensions can be fused together. For example, it is theoretically possible to incorporate up to 256 polarization dimensions to the OAM-CCL using commercially available spatial light modulators, and we predict that the security of the OAM-CCL-based communication system will be further improved[48] (legal BER $< 10^{-4}$ and illegal BER $\gg$ FEC), and the system capacity can theoretically reach the order of 66.56 Tb/s[33] (26 OAM $\times$ 256 Pol.), while the requirements of the system on the environment to be more loosened. In addition, we simulate the communication performance of the system under turbulent conditions, details of which are given in Fig. S16 in the Supplementary Material. The results show that the system still performs well under the moderately turbulent condition, meaning that the system has the potential to be used in a variety of environments, such as underwater and atmospheric.

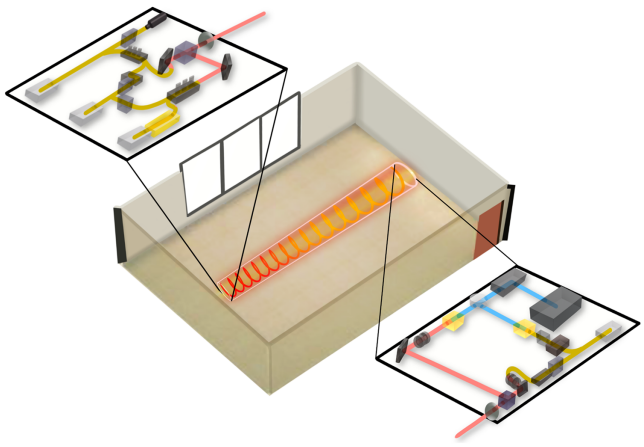

Fig. 6 Illustration of the indoor communication simulation for the OAM-CCL-based communication system.

In order to improve the robustness of chaotic synchronization, we use the commonly driven chaotic synchronization mechanism as the core of the encryption and decryption mechanism in the OAM-CCL-based communication system. Interestingly, the OAM modes allow the OAM-CCL-based communication system to have multiple channels, so we can use different channels to transmit the driving chaotic signal and the encrypted signal, respectively, reducing the interference between each other, thus improving the quality of chaotic synchronization.

So far, the OAM-CCL-based communication system is in its infancy. Its practical implementation still faces several significant challenges, including beam divergence, alignment issues, atmospheric turbulence, and the lack of standardized protocol and interface. Therefore, in future endeavors, it is crucial to integrate the OAM-CCL-based communication with beam shaping technology,[49] adaptive optics technology,[50] and a tracking and capture system[51] to overcome the challenges posed by divergence, misalignment, and turbulence. Furthermore, there is a pressing necessity to formulate communication protocol standards aimed at augmenting interoperability and compatibility between the OAM-CCL-based communication system and the established optical communication infrastructure.

Our team has done extensive preliminary research on chaotic secure communication and OAM light beams, respectively. The former mainly includes long-range chaotic synchronization,[52] chaotic lasers for high-speed classical key distribution,[53] and coherent chaotic optical communication.[37] The latter mainly consists of OAM generation,[54] manipulation,[29] and application.[30,31,33] These above achievements have laid a solid foundation for the experimental realization of OAM-CCL and OAM-CCL-based communication systems. As a result, we believe it is reasonable to use the conceptual paradigm of OAM-CCL to establish a

superior-security, massive-capacity, high-fidelity, and robust optical communication.

4 Conclusions

To conclude, we have theoretically presented and experimentally verified a new conceptual paradigm for the generation of OAM-CCL supporting access to high-security and massive-capacity optical communications. To achieve this, we first leverage the spatial light modulator to encode the OAM of the chaotic laser, and then regard it as an ultrabandwidth source to drive synchronous mask for communicating in free space. It is shown that the use of OAM-CCL carrying 11 vortex modes enables to succeed in achieving a versatile optical communication system, which features a total transmission capacity of 100 Gb/s and a bit error rate below the FEC threshold 3.8×10^{-3}. In addition, such an OAM-CCL-based communication system is nearly immune to the 3D misalignment within the prescribed argument scopes. It is worth mentioning that the OAM modes allow the OAM-CCL system to have multiple channels, so it is well suited to the commonly driven chaotic synchronization mechanism.

Compared to the existing communication technologies (traditional free-space optical communication or chaotic optical communication), our proposed system is primarily distinguished by both high security and massive capacity. On the one hand, the fusion of temporal chaotic signal and spatial OAM beam ensures the multidimensional encryption of the OAM-CCL-based communication system, making it difficult to eavesdrop, separate, and decrypt. On the other hand, because of the engagement of spatial OAM modes, the OAM-CCL-based communication system is shown to exhibit unlimited storage capacity and superior compatibility in principle. As a result, it is expected to potentially achieve Pb/s capacity by combining with techniques, such as wavelength division multiplexing, advanced modulation, and fractional OAM, although we only show a 100 Gb/s level in this article as a fundamental illustration. In addition, in order to further improve the antimisalignment ability of the OAM-CCL-based communication system, we may resort to some additional techniques, such as power adaptive compensation, demasking power matching, and a tracking system, thus forecasting that the misalignment error rate will drop to a lower level. Beyond that, the OAM-CCL-based communication system is based on an all-optical feedback chaotic laser, which means that it is easy to integrate into large-scale high-rate optical communication networks. The conceptual paradigm for OAM-CCL provides a feasible idea for high-security, large-capacity, and robust optical communications.

Disclosures

The authors declare no conflicts of interest.

Code and Data Availability

Data underlying the results presented in this paper are not publicly available at this time but may be obtained from the authors upon reasonable request.

Acknowledgments

This work was supported by the National Natural Science Foundation of China (Grant Nos. 61927811, 62035009, and 11974258), the Fundamental Research Program of Shanxi Province (Grant No. 202103021224038), the Development Fund in Science and Technology of Shanxi Province (Grant No. YDZJSX2021A009), the Open Fund of State Key Laboratory of Applied Optics (Grant No. SKLAO2022001A09), the Science and Technology Foundation of Guizhou Province (Grant Nos. ZK [2021]031 and ZK [2023] 049), and the Program for Guangdong Introducing Innovative and Entrepreneurial Teams.

References

1. M. Sciamanna and K. A. Shore, "Physics and applications of laser diode chaos," *Nat. Photonics* **9**(3), 151–162 (2015).
2. A. Argyris et al., "Chaos-based communications at high bit rates using commercial fibre-optic links," *Nature* **438**(7066), 343–346 (2005).
3. E. Klein et al., "Public-channel cryptography using chaos synchronization," *Phys. Rev. E* **72**(1), 016214 (2005).
4. M. Zhang et al., "Generation of broadband chaotic laser using dual-wavelength optically injected Fabry–Pérot laser diode with optical feedback," *IEEE Photonics Technol. Lett.* **23**(24), 1872–1874 (2011).
5. L. Qiao et al., "Generation of flat wideband chaos based on mutual injection of semiconductor lasers," *Opt. Lett.* **44**, 5394–5397 (2019).
6. R. Lavrov, M. Jacquot, and L. Larger, "Nonlocal nonlinear electro-optic phase dynamics demonstrating 10 Gb/s chaos communications," *IEEE J. Quantum Electron.* **46**(10), 1430–1435 (2010).
7. Q. Yang et al., "Generation of a broadband chaotic laser by active optical feedback loop combined with a high nonlinear fiber," *Opt. Lett.* **45**, 1750–1753 (2020).
8. P. Li et al., "Observation of flat chaos generation using an optical feedback multi-mode laser with a band-pass filter," *Opt. Express* **27**, 17859–17867 (2019).
9. N. Jiang et al., "Physical secure optical communication based on private chaotic spectral phase encryption/decryption," *Opt. Lett.* **44**, 1536–1539 (2019).
10. N. Li et al., "Enhanced two-channel optical chaotic communication using isochronous synchronization," *IEEE J. Sel. Top. Quantum Electron.* **19**(4), 0600109 (2012).
11. M. Cheng et al., "Security-enhanced OFDM-PON using hybrid chaotic system," *IEEE Photonics Technol. Lett.* **27**(3), 326–329 (2014).
12. X. Dou et al., "Experimental demonstration of polarization-division multiplexing of chaotic laser secure communications," *Appl. Opt.* **54**, 4509–4513 (2015).
13. J. Ke et al., "Chaotic optical communications over 100-km fiber transmission at 30-gb/s bit rate," *Opt. Lett.* **43**(6), 1323–1326 (2018).
14. A. Zhao et al., "Physical layer encryption for WDM optical communication systems using private chaotic phase scrambling," *J. Lightwave Technol.* **39**(8), 2288–2295 (2021).
15. Y. Fu et al., "High-speed optical secure communication with an external noise source and an internal time-delayed feedback loop," *Photonics Res.* **7**(11), 1306–1313 (2019).
16. J. Ai, L. Wang, and J. Wang, "Secure communications of CAP-4 and OOK signals over MMF based on electro-optic chaos," *Opt. Lett.* **42**, 3662–3665 (2017).
17. J. Wang et al., "Terabit free-space data transmission employing orbital angular momentum multiplexing," *Nat. Photonics* **6**(7), 488–496 (2012).
18. H. Huang et al., "100 tbit/s free-space data link enabled by three-dimensional multiplexing of orbital angular momentum, polarization, and wavelength," *Opt. Lett.* **39**(2), 197–200 (2014).
19. J. Wang et al., "N-dimentional multiplexing link with 1.036-Pbit/s transmission capacity and 112.6-bit/s/Hz spectral efficiency using OFDM-8QAM signals over 368 WDM pol-muxed 26 OAM modes," in *Eur. Conf. Opt. Commun. (ECOC)*, pp. 1–3 (2014).

20. Y. Ren et al., "Experimental characterization of a 400 Gbit/s orbital angular momentum multiplexed free-space optical link over 120 m," *Opt. Lett.* **41**(3), 622–625 (2016).
21. K. Zou et al., "High-capacity free-space optical communications using wavelength-and mode-division-multiplexing in the mid-infrared region," *Nat. Commun.* **13**(1), 7662 (2022).
22. K. Zhang et al., "A review of orbital angular momentum vortex beams generation: from traditional methods to metasurfaces," *Appl. Sci.* **10**(3), 1015 (2020).
23. B. Dutta et al., "Numerical evaluation of bidirectional high-speed data transmission over turbulence tolerable FSO link employing WDM-OAM multiplexing and DP-QPSK modulation techniques," *Opt. Commun.* **546**, 129753 (2023).
24. B. Dutta et al., "100 Gbps data transmission based on different l-valued OAM beam multiplexing employing WDM techniques and free space optics," *Opt. Quantum Electron.* **53**(9), 515 (2021).
25. B. Dutta et al., "640 Gbps FSO data transmission system based on orbital angular momentum beam multiplexing employing optical frequency comb," *Opt. Quantum Electron.* **54**(2), 132 (2022).
26. K. Dholakia and T. Čižmár, "Shaping the future of manipulation," *Nat. Photonics* **5**(6), 335–342 (2011).
27. M. P. MacDonald et al., "Creation and manipulation of three-dimensional optically trapped structures," *Science* **296**(5570), 1101–1103 (2002).
28. L. Paterson et al., "Controlled rotation of optically trapped microscopic particles," *Science* **292**(5518), 912–914 (2001).
29. S. Lin et al., "All-optical vectorial control of multistate magnetization through anisotropy-mediated spin-orbit coupling," *Nanophotonics* **8**(12), 2177–2188 (2019).
30. Y. Zhang et al., "Ultrafast multi-target control of tightly focused light fields," *Opto-Electron. Adv.* **5**(3), 210026 (2022).
31. Y. Zhang et al., "Dual-point noncoaxial rotational Doppler effect towards synthetic OAM light fields for real-time rotating axis detection," *Light: Adv. Manuf.* **4**, 1–11 (2023).
32. S. Bernet et al., "Quantitative imaging of complex samples by spiral phase contrast microscopy," *Opt. Express* **14**(9), 3792–3805 (2006).
33. Z.-Q. Nie et al., "Three-dimensional super-resolution longitudinal magnetization spot arrays," *Light Sci. Appl.* **6**(8), e17032 (2017).
34. R. Lang and K. Kobayashi, "External optical feedback effects on semiconductor injection laser properties," *IEEE J. Quantum Electron.* **16**(3), 347–355 (1980).
35. A. Wang, Y. Wang, and J. Wang, "Route to broadband chaos in a chaotic laser diode subject to optical injection," *Opt. Lett.* **34**(8), 1144–1146 (2009).
36. T. Yamamoto et al., "Common-chaotic-signal induced synchronization in semiconductor lasers," *Opt. Express* **15**(7), 3974–3980 (2007).
37. L. Wang et al., "Scheme of coherent optical chaos communication," *Opt. Lett.* **45**(17), 4762–4765 (2020).
38. J. Liu, J. Zhang, and Y. Wang, "Secure communication via chaotic synchronization based on reservoir computing," *IEEE Trans. Neural Networks Learn. Syst.* **35**, 285–299 (2022).
39. M. Zhang and Y. Wang, "Review on chaotic lasers and measurement applications," *J. Lightwave Technol.* **39**(12), 3711–3723 (2021).
40. A. Sawant et al., "Ultimate capacity analysis of orbital angular momentum channels," *IEEE Wireless Commun.* **28**(1), 90–96 (2020).
41. R. L. Phillips and L. C. Andrews, "Spot size and divergence for Laguerre Gaussian beams of any order," *Appl. Opt.* **22**(5), 643–644 (1983).
42. P. Vaveliuk, B. Ruiz, and A. Lencina, "Limits of the paraxial approximation in laser beams," *Opt. Lett.* **32**(8), 927–929 (2007).
43. G. Molina-Terriza, J. P. Torres, and L. Torner, "Management of the angular momentum of light: preparation of photons in multidimensional vector states of angular momentum," *Phys. Rev. Lett.* **88**(1), 013601 (2001).
44. Y.-D. Liu et al., "Orbital angular momentum (OAM) spectrum correction in free space optical communication," *Opt. Express* **16**(10), 7091–7101 (2008).
45. G. Xie et al., "Performance metrics and design considerations for a free-space optical orbital-angular-momentum–multiplexed communication link," *Optica* **2**(4), 357–365 (2015).
46. M. Vasnetsov, V. Pas' Ko, and M. Soskin, "Analysis of orbital angular momentum of a misaligned optical beam," *New J. Phys.* **7**(1), 46 (2005).
47. J. Cao et al., "Mitigating the cross talk of orbital angular momentum modes in free-space optical communication by using an annular vortex beam and a focusing mirror," *Front. Phys.* **10** (2022).
48. X. Li et al., "Three-dimensional orientation-unlimited polarization encryption by a single optically configured vectorial beam," *Nat. Commun.* **3**(1), 998 (2012).
49. L. Li et al., "Orbital-angular-momentum-multiplexed free-space optical communication link using transmitter lenses," *Appl. Opt.* **55**(8), 2098–2103 (2016).
50. Y. Ren et al., "Adaptive-optics-based simultaneous pre-and post-turbulence compensation of multiple orbital-angular-momentum beams in a bidirectional free-space optical link," *Optica* **1**(6), 376–382 (2014).
51. G. Xie et al., "Localization from the unique intensity gradient of an orbital-angular-momentum beam," *Opt. Lett.* **42**(3), 395–398 (2017).
52. L. Wang et al., "Chaos synchronization of semiconductor lasers over 1040-km fiber relay transmission with hybrid amplification," *Photonics Res.* **11**(6), 953–960 (2023).
53. H. Gao et al., "0.75 Gbit/s high-speed classical key distribution with mode-shift keying chaos synchronization of Fabry–Perot lasers," *Light Sci. Appl.* **10**(1), 172 (2021).
54. X. Wang et al., "Recent advances on optical vortex generation," *Nanophotonics* **7**(9), 1533–1556 (2018).
55. Z. Wang et al., "Image quality assessment: from error visibility to structural similarity," *IEEE Trans. Image Process.* **13**(4), 600–612 (2004).
56. J. Xu, "Degrees of freedom of OAM-based line-of-sight radio systems," *IEEE Trans. Antennas Propag.* **65**(4), 1996–2008 (2017).
57. X. Sun and I. B. Djordjevic, "Physical-layer security in orbital angular momentum multiplexing free-space optical communications," *IEEE Photonics J.* **8**(1), 7901110 (2016).
58. S. Franke-Arnold et al., "Uncertainty principle for angular position and angular momentum," *New J. Phys.* **6**(1), 103 (2004).
59. M. Bloch et al., "Wireless information-theoretic security," *IEEE Trans. Inf. Theory* **54**(6), 2515–2534 (2008).

Yanwei Cui received his BS degree in measurement and control technology and instrumentation from Qingdao University of Science and Technology, Qingdao, China, in 2021. He is currently pursuing his MS degree in instrument science and technology at Taiyuan University of Technology, Taiyuan, China. His research interests include information security and chaotic secure communication.

Jianguo Zhang received his BS degree in automation, his MS degree in detection technology and automatic equipment, and his PhD in circuit and system from Taiyuan University of Technology, Taiyuan, China, in 2002, 2005, and 2013, respectively. He is currently an associate professor at the Key Laboratory of Advanced Transducers and Intelligent Control System of Taiyuan University of Technology. His research interests include information security technology, deep learning, and hardware implementation of neural networks.

Zhongquan Nie is an associate research fellow of the College of Advanced Interdisciplinary Studies at the National University of Defense Technology, Changsha, China. He obtained his PhD in physics in 2015 from Harbin Institute of Technology, Harbin, China. His research fields

include structure vector light field control, all-optical magnetic recording/storage, interaction between light and matter, and femtosecond laser direct writing. He has published 70 papers in journals, such as *Light: Science and Applications*, *Science Advances*, *Opto-Electronic Advances*, *Light: Advanced Manufacturing*, and *Advanced Photonics Nexus*.

Anbang Wang received his BS degree in applied physics and his PhD in electronic circuits and systems from Taiyuan University of Technology, Taiyuan, China, in 2003 and 2014, respectively. He is currently a professor at the School of Information Engineering of Guangdong University of Technology, Guangzhou, China. His research interests include laser dynamics, wideband chaos generation, optical time-domain reflectometry, random bit generation, and secure communications.

Yuncai Wang received his BS degree in semiconductor physics from Nankai University, Tianjin, China, in 1986, and his MS and PhD degrees in physics and optics from Xi'an Institute of Optics and Precision Mechanics, Chinese Academy of Sciences, Xi'an, China, in 1994 and 1997, respectively. He is currently the deputy director of the Advanced Institute of Photonic Technology at the Guangdong University of Technology. His research interests include nonlinear dynamics of semiconductor lasers and chaotic secure communication.